

Multi-wavelength Dark Matter signals from the Galaxy

Alessandro Cuoco,
Oskar Klein Center,
Stockholm University



GGI Workshop,
May 7th 2010



Indirect Detection of Dark Matter: the General Framework

1) WIMP Annihilation

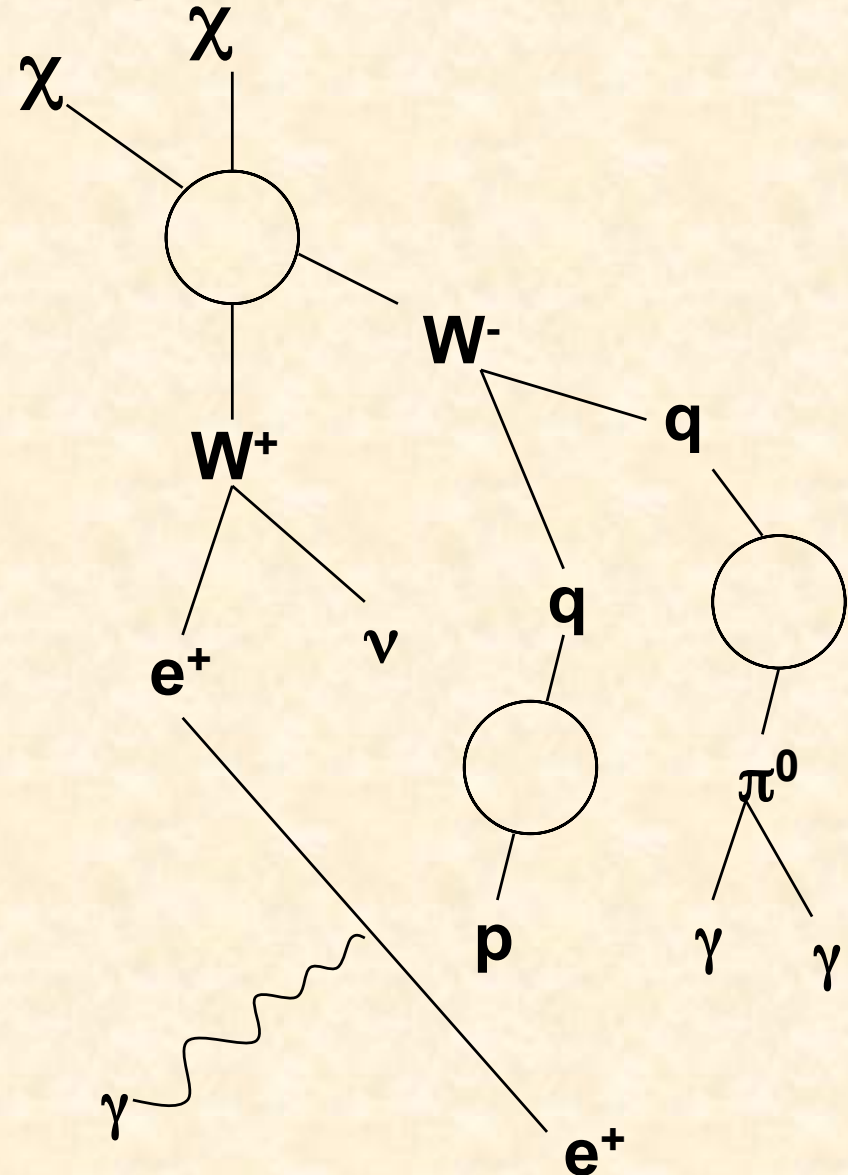
Typical final states include heavy fermions, gauge or Higgs bosons

2) Fragmentation/Decay

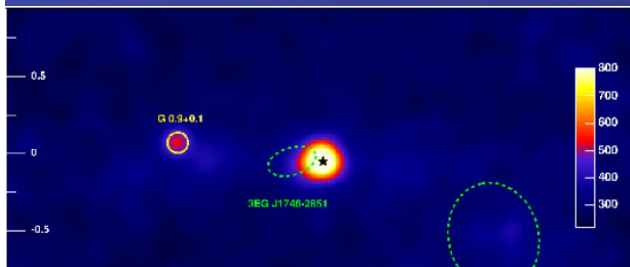
Annihilation products decay and/or fragment into some combination of electrons, protons, deuterium, neutrinos and gamma rays

3) Synchrotron and Inverse Compton

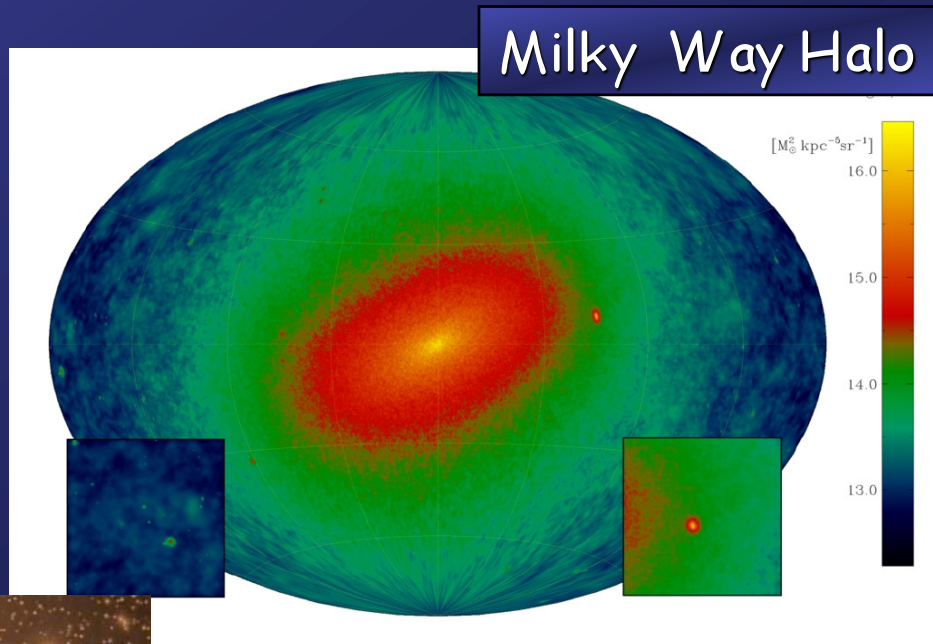
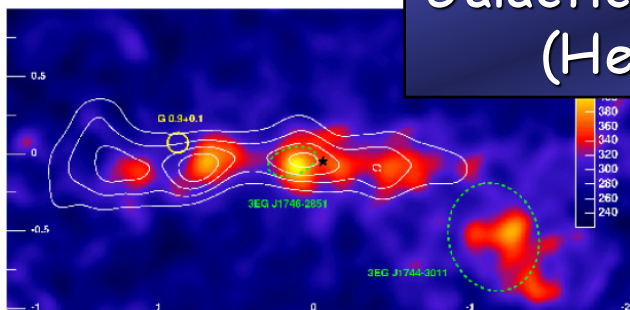
Relativistic electrons up-scatter starlight to MeV-GeV energies, and emit synchrotron photons via interactions with magnetic fields



Where to look



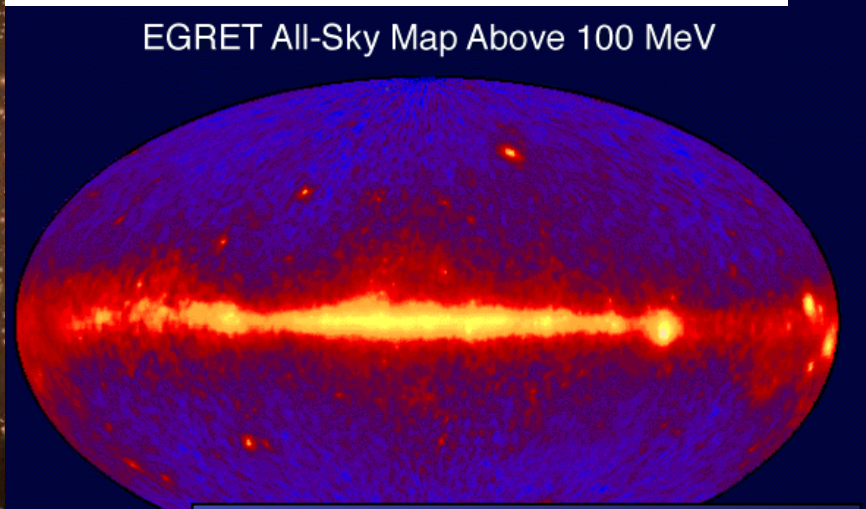
Galactic Center
(Hess)



Milky Way Halo

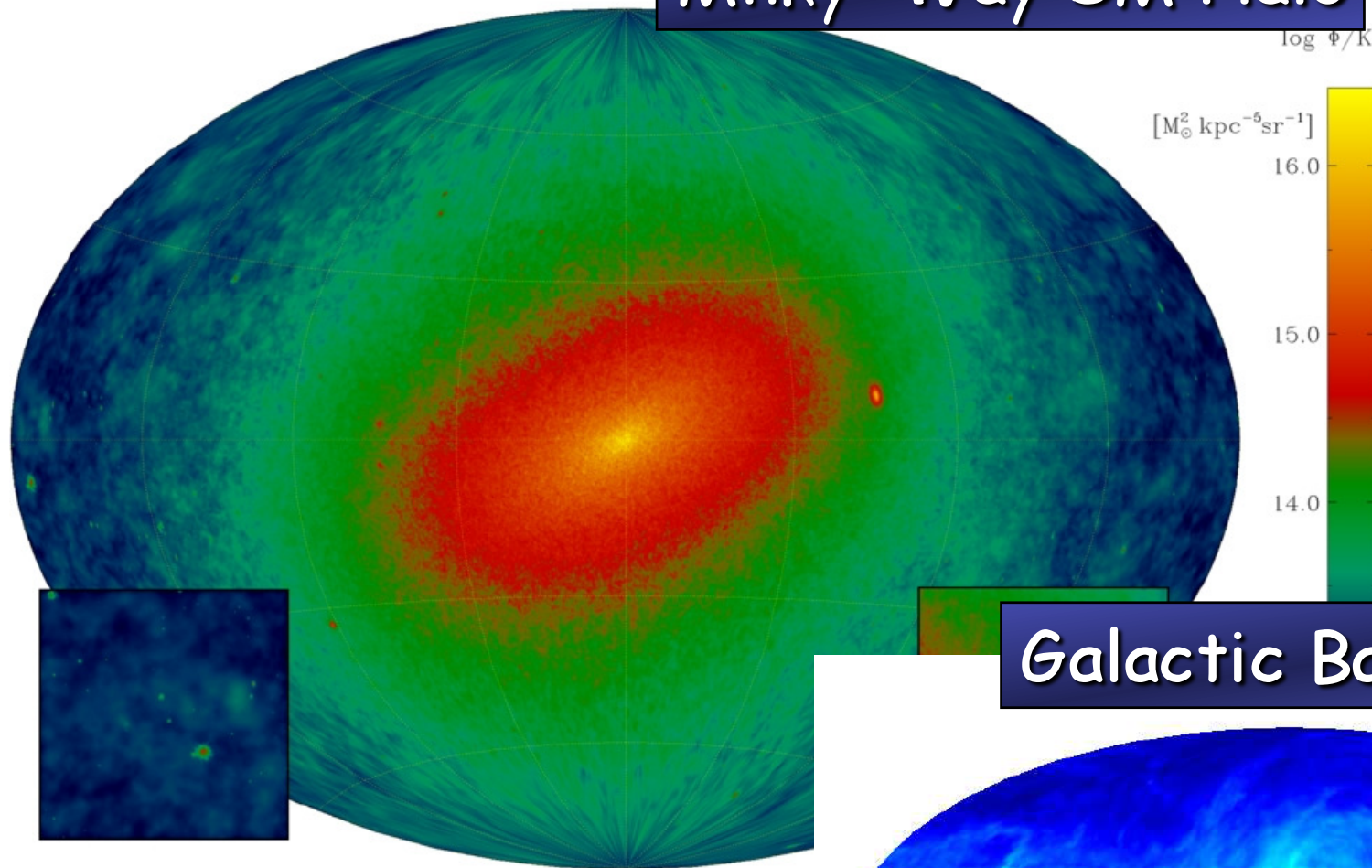


DM Clumps:
Via Lactea
Simulation
Diemand et al.

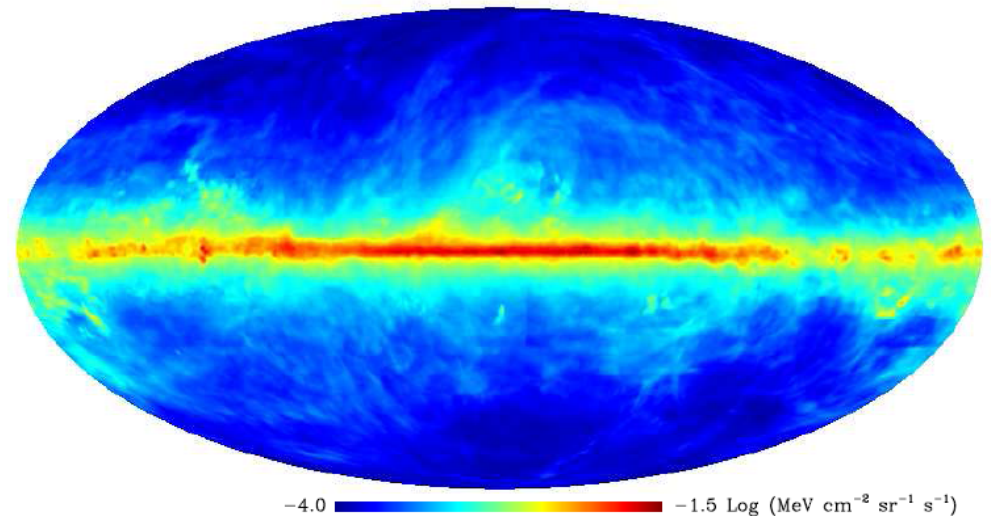


Extra Galactic
Background

Milky Way DM Halo



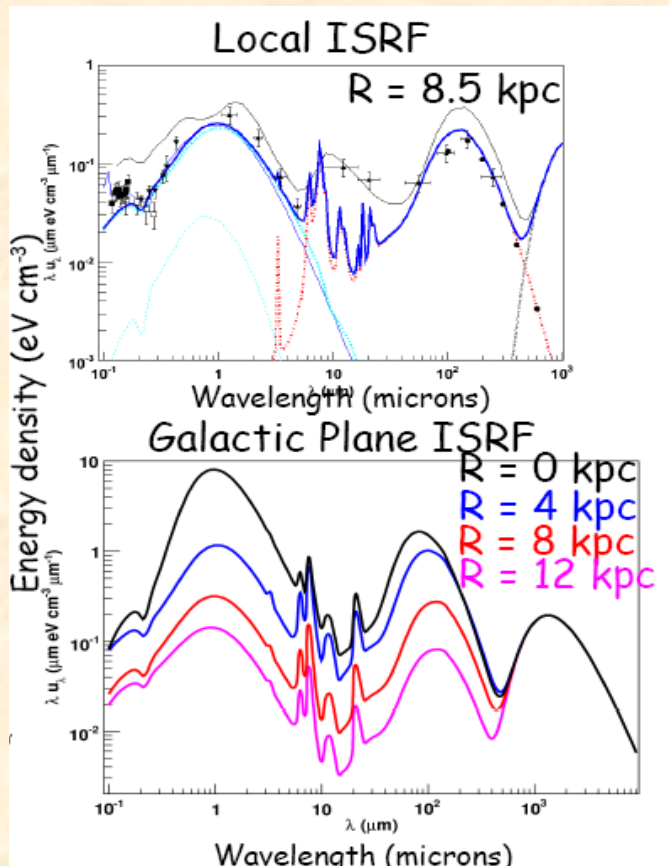
Galactic Backgrounds



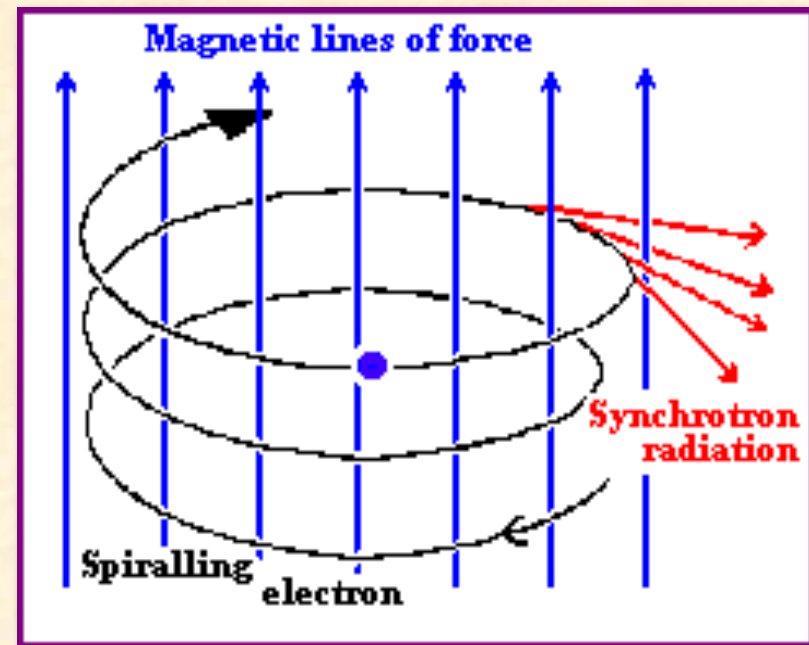
Different morphologies can be exploited to disentangle the DM signal from astrophysics

Indirect Detection With Synchrotron and Inverse Compton Radiation

ICS on the Galactic ISRF



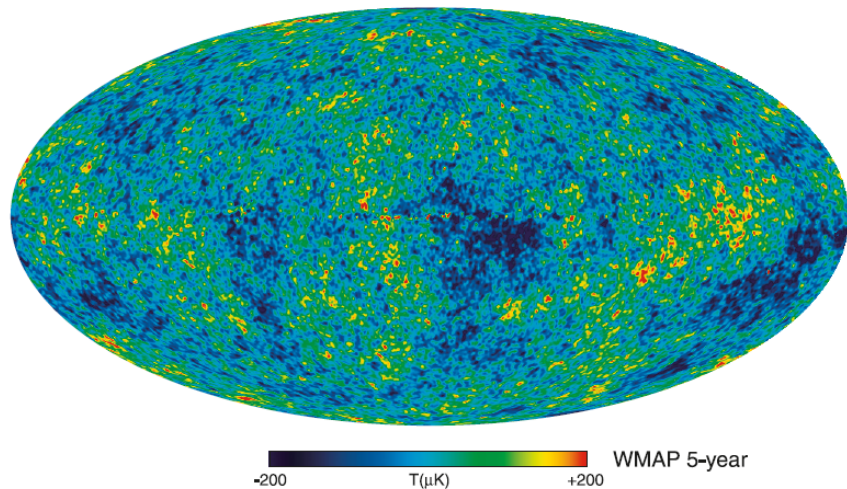
Synchrotron on the GMF



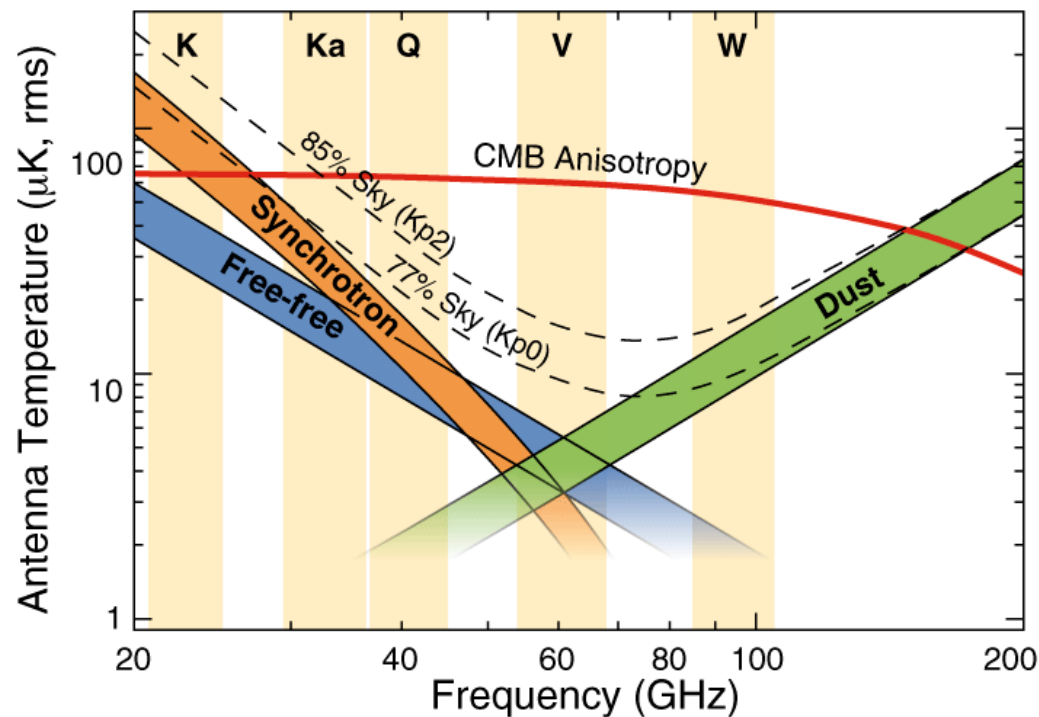
- Charged leptons and nuclei strongly interact with gas, Interstellar Radiation and Galactic Magnetic Field.
- During the process of thermalization **HE $e+e^-$** release secondary low energy radiation, in particular in the **radio and X-ray/soft Gamma** band.

Milky Way Halo and Secondary Radiation: synchrotron

The Microwave sky



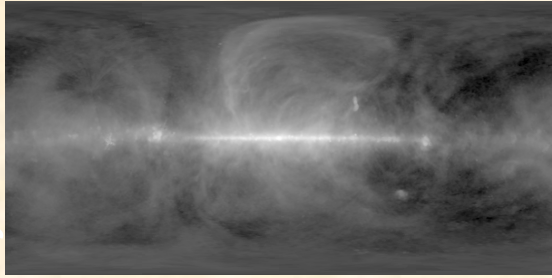
- In addition to CMB photons, WMAP data is "contaminated" by a number of galactic foregrounds that must be accurately subtracted



- The WMAP frequency range is well suited to minimize the impact of foregrounds

- Substantial challenges are involved in identifying and removing foregrounds

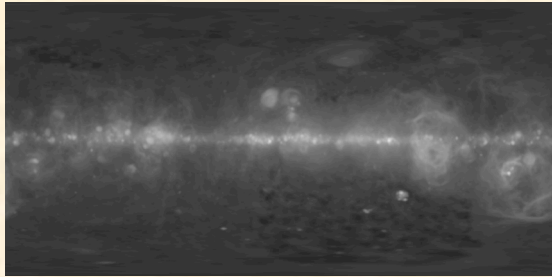
Synchrotron



Synchrotron: Template: C.G.T. Haslam et al., A & A **100 (1981) 209.**

+

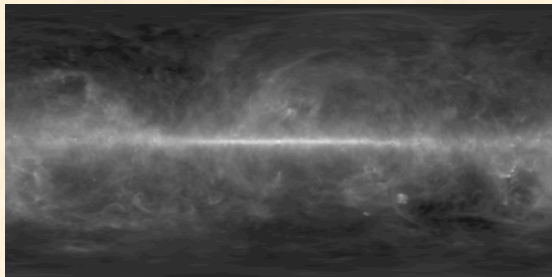
Free-free



Freefree: Template: D.P. Finkbeiner, ApJS **146 (2003) 407.**

+

T & S Dust

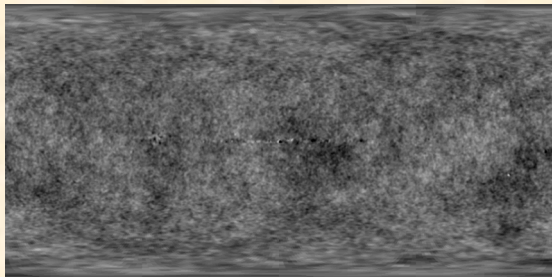


Dust: Template: D.P. Finkbeiner et al., ApJ **524 (1999) 867.**

WMAP

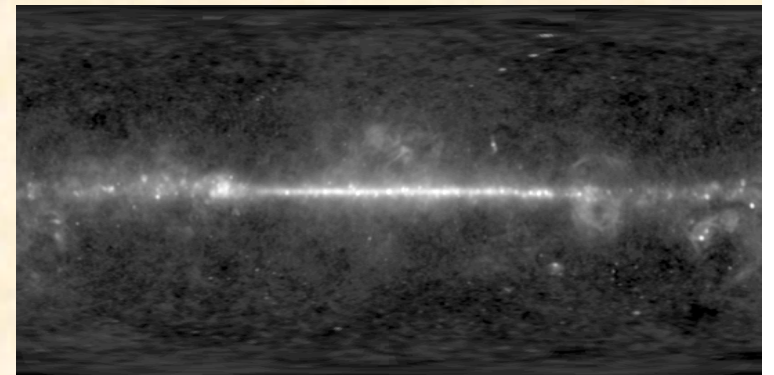
+

CMB

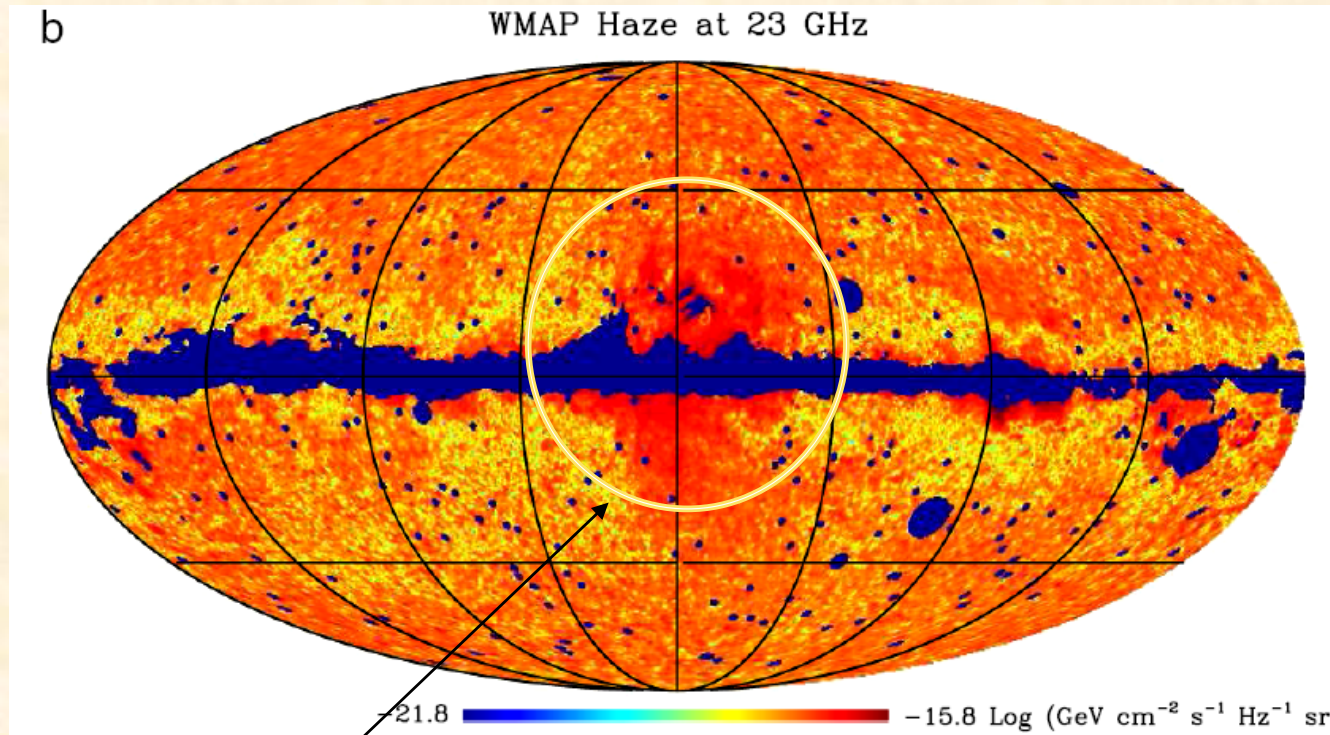


CMB: Gold et al.,
arXIV:1001.4555.

TOTAL



The "WMAP Haze"



After known foregrounds are subtracted, an excess appears in the residual maps within the inner $\sim 20^\circ$ around the Galactic Center

D. P. Finkbeiner, *Astrophys. J.* 614 (2004) 186

G. Dobler and D. P. Finkbeiner, arXiv:0712.1038 [astro-ph].

The “WMAP Haze” by the WMAP Team

The fit procedure used for the haze extraction is quite important, and using more degrees of freedom to model the foregrounds as performed by the WMAP team fails in finding the feature. They still find an hardening of the synchrotron emission in the Haze region, though.

Map of the synchrotron spectral indexes in a pixel by pixel fit procedure by WMAP

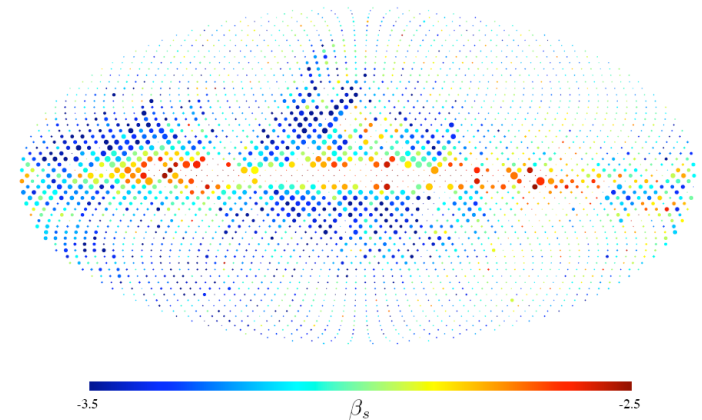
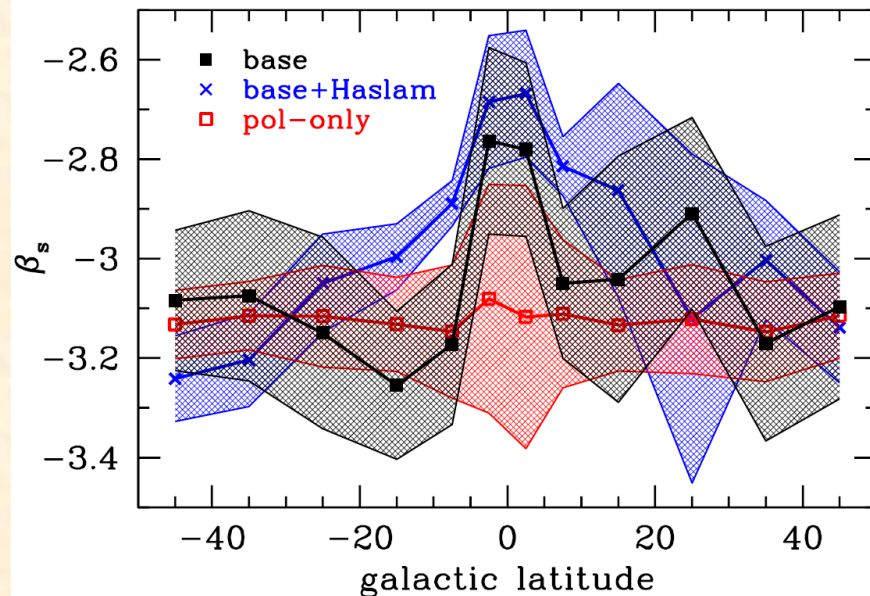


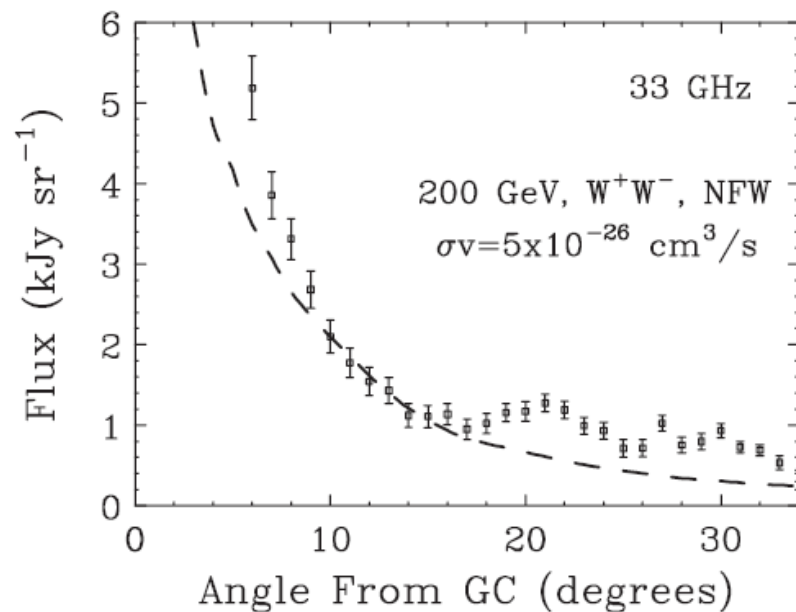
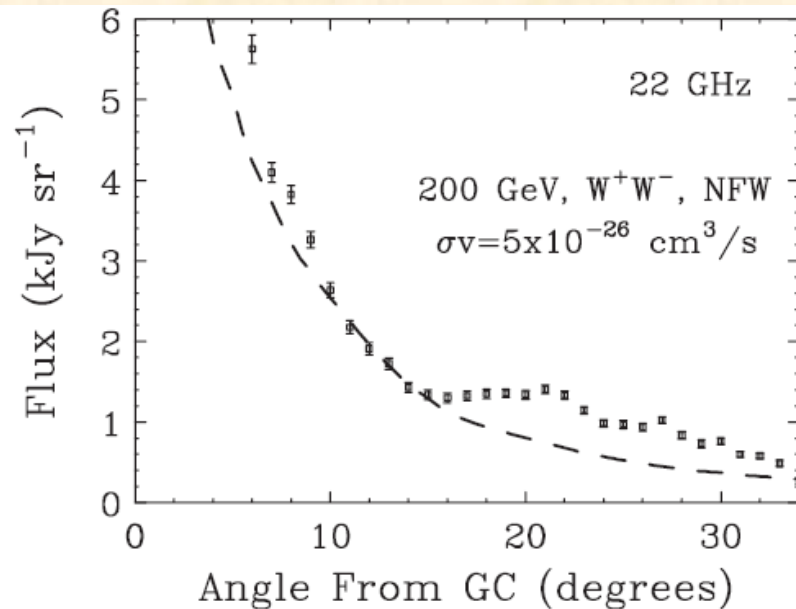
Fig. 11.— Map of synchrotron spectral index for the “base” fit, binned to $N_{\text{side}} = 16$. Color shows the value of the spectral index, and circle area indicates the weight σ_{β}^{-2} given by the fit. Pixels with $\chi_p^2 > 2$ were explicitly de-weighted.

Synchrotron spectral indexes averaged along constant longitudes stripes by WMAP



WMAP Collaboration (B. Gold et al.) 2008
[arXiv:astro-ph/0803.0715].
D.T. Cumberbatch,, arXiv:0902.0039 [astro-ph].

DM Fit of the Haze Fit

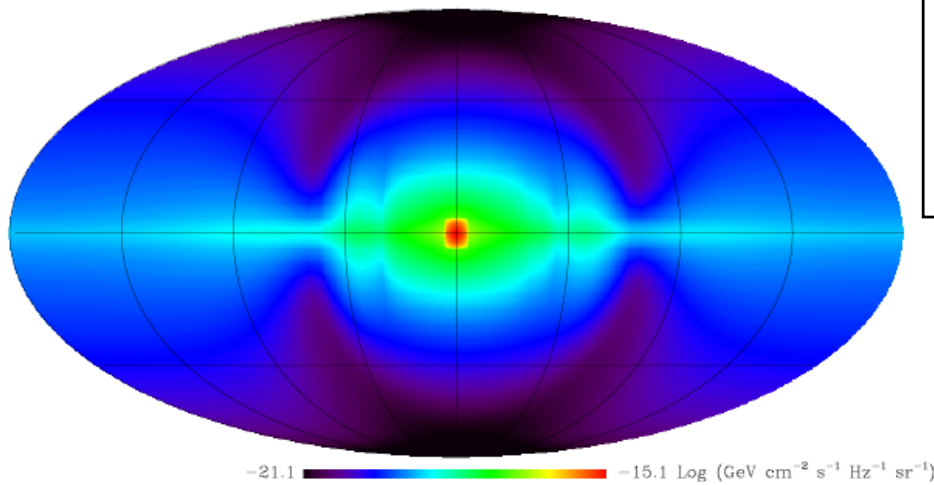


Haze Fit: Hooper, 2007, Hooper et al. 2008

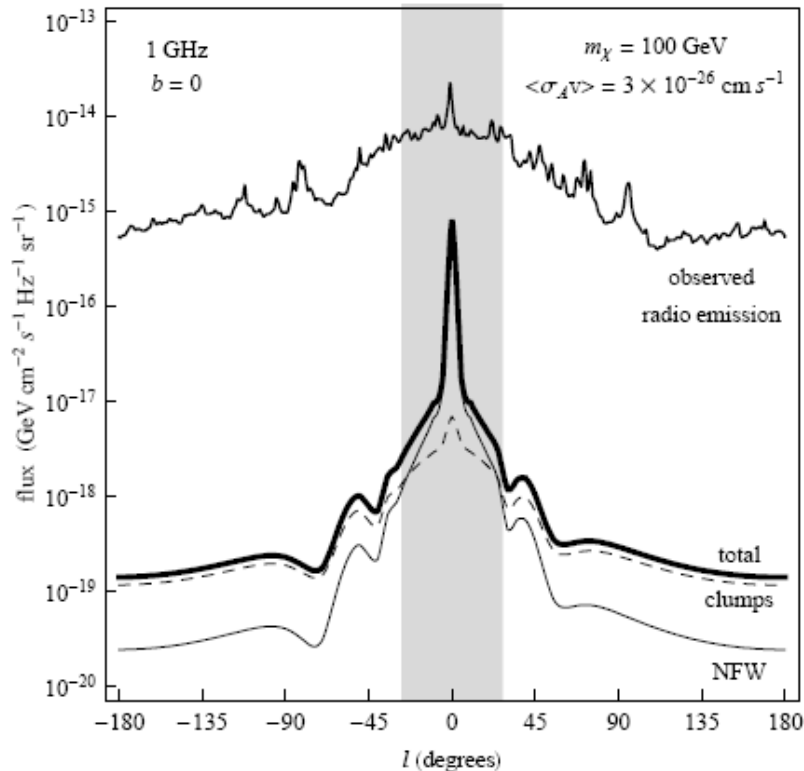
Averaged Haze Profile at 22 and 33 GHz bands, as a function of the angle from the Galactic Center and flux of synchrotron emission from the annihilation products of a 200 GeV neutralino annihilating to WW . A constant ratio $U_b/(U_b + U_{rad}) = 0,26$ is employed.

DM diffuse signal

DM synchrotron at 1 GHz



Pattern of the DM synchrotron emission at 1 GHz. The characteristic pattern is given by the line of sight projection of the galactic magnetic field.

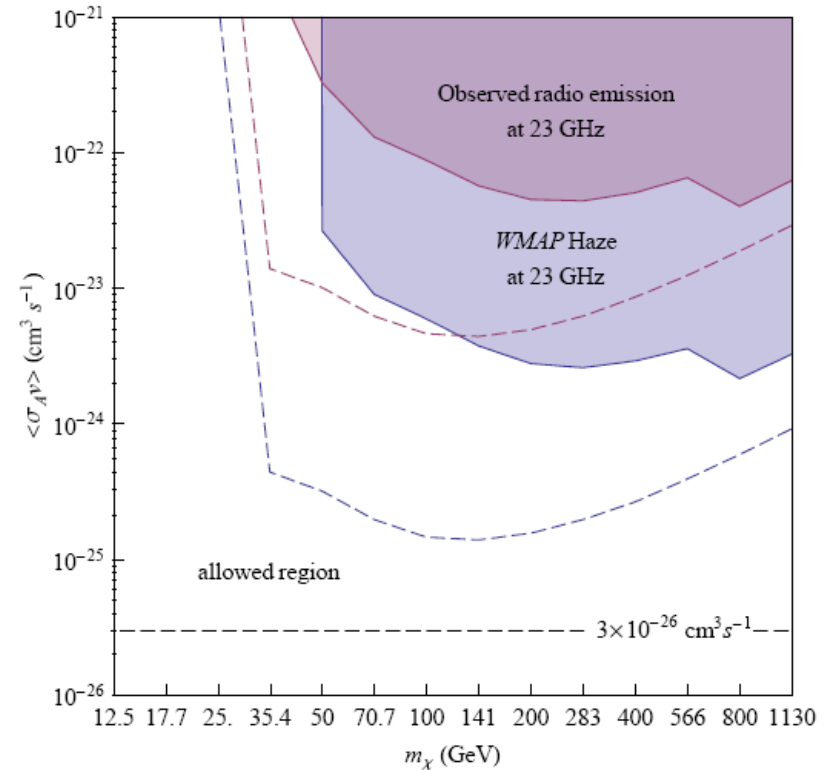
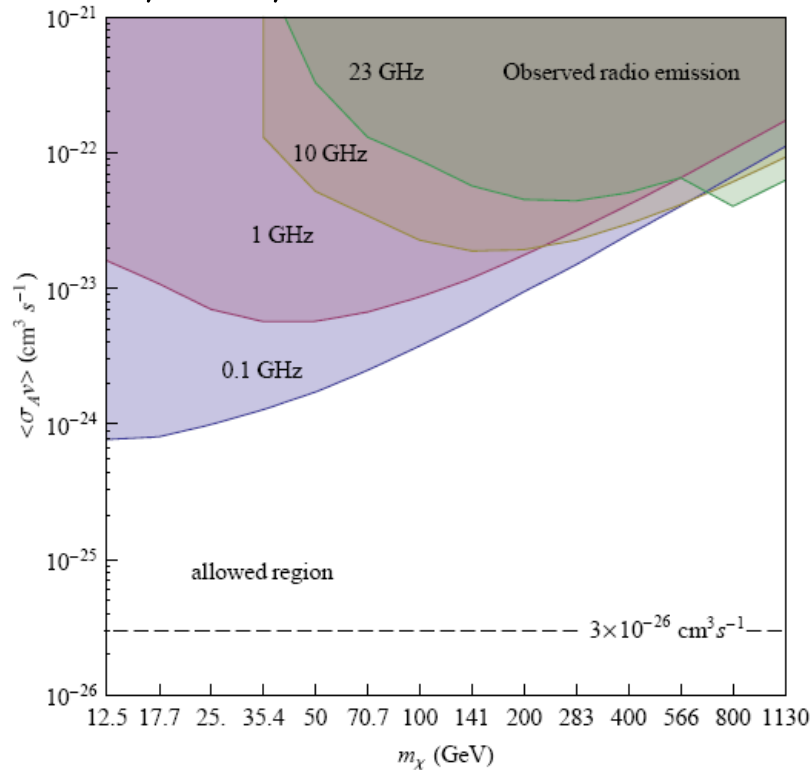


Requiring that the DM signal does not exceed the observed radio emission (CMB cleaned, but not foreground cleaned) DM constraints in the $m_{\chi} - \langle \sigma_{AV} \rangle$ plane can be derived. The region around the GC ($15^{\circ} \times 15^{\circ}$) is excluded from the analysis.

DM synchrotron profile for the halo and unresolved substructures and their sum at 1 GHz. The astrophysical observed emission at the same frequency is also shown. The gray band indicates the angular region within which the DM signal from the host halo dominates over the signal from substructures

DM constraints in the $m_\chi - \langle \sigma_{A\nu} \rangle$ plane

Borriello, Cuoco, Miele 2008

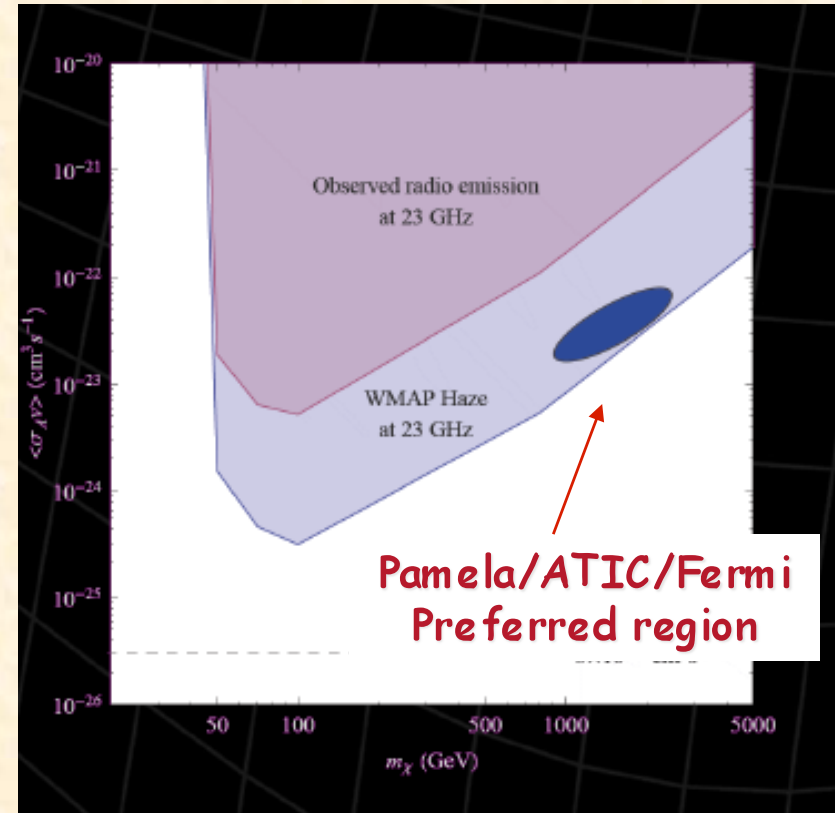
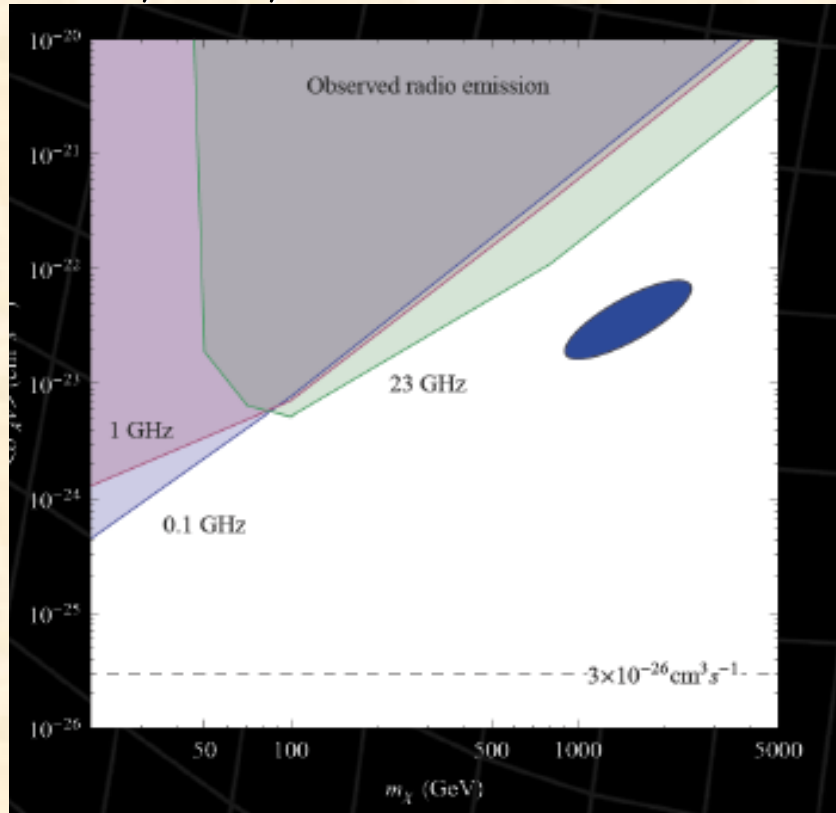


- Constraints in the $m_\chi - \langle \sigma_{A\nu} \rangle$ plane for various frequencies, without assuming synchrotron foreground removal.
- DM spectrum is harder than background, thus constraints are better at lower frequencies.

- Constraints from the WMAP 23 GHz foreground map and 23 GHz foreground cleaned residual map (the WMAP Haze) for the TT model of magnetic field (filled regions) and for a uniform $10 \mu\text{G}$ field (dashed lines).
- With a fine tuning of the MF is possible to adjust the DM signal so that to match the Haze, like in Hooper et al.

Same for $\mu+\mu^-$ channel

Borriello, Cuoco, Miele 2008



Lower limit for the magnetic field near the GC

$$\nu_b = \nu_b(n_H, B) \approx 1.7 \text{ GHz}$$

$$B \simeq B(n_H)$$

$$\frac{dN_e}{dE_e} \propto E_e^p$$

$$\frac{dn_e}{dE_e}(n_H, B, p)$$

$$F_\nu^{(brm+ICS)}(n_H, B, p)$$

$$F_\nu^{(syn)}(n_H, B, p)$$

$$F_\nu^{(brm+ICS)} \leq F_\nu^{(Hess)}$$

$$B \gtrsim 50 \mu\text{G}$$

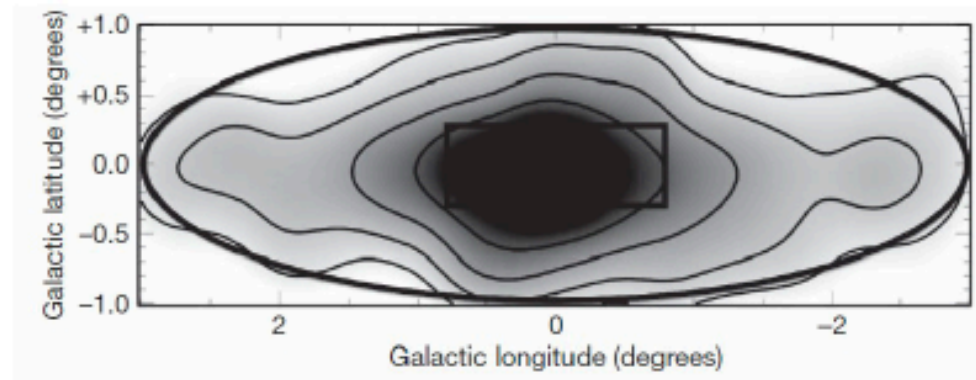
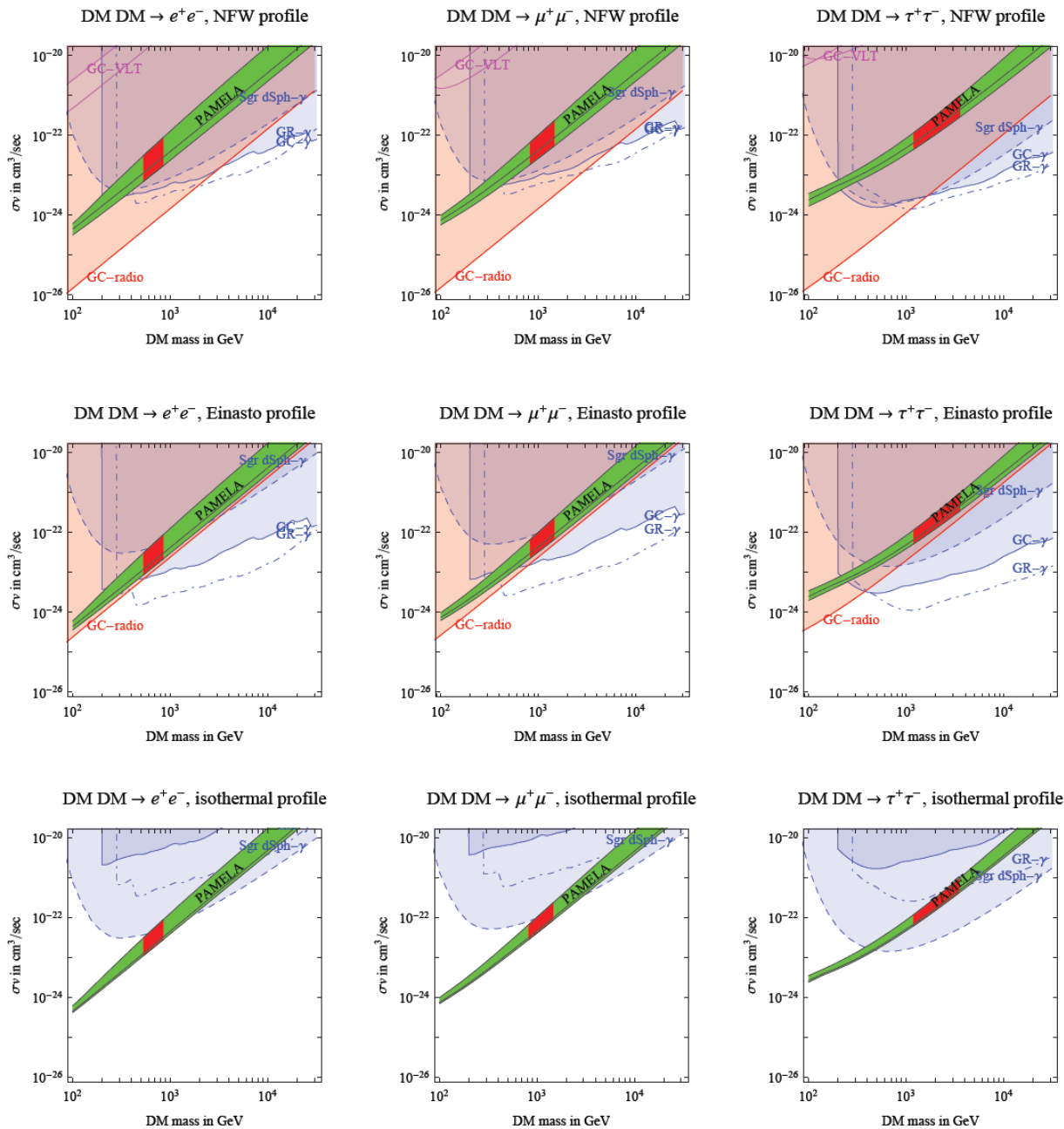


Figure 1 | Total intensity image of the region at 10 GHz. Radio map¹³ convolved to a resolution of $1.2^\circ \times 1.2^\circ$ with contours at 10, 20, 40, 80, 160 and 240 Jy per beam. (Native resolution and convolved images at $\nu \geq 1.4$ GHz are available in the Supplementary Information.) There is a striking constancy in the appearance of the radio structure from 74 MHz to at least 10 GHz (the large ellipse traces the diffuse, non-thermal radio emission region first identified at 74 and 330 MHz; ref. 6). The small rectangle delineates the region from which the HESS collaboration determines a diffuse \sim TeV γ -ray intensity⁸.

DM constraints from the Galactic Center



More stringent constraints but more model dependent on the DM profile and magnetic field in the GC

G. Bertone, M. Cirelli, A. Strumia, M. Taoso, JCAP 2009, arXiv: 0811.3744

The Future: SKA and PLANCK



PLANCK

Launch: June 2009

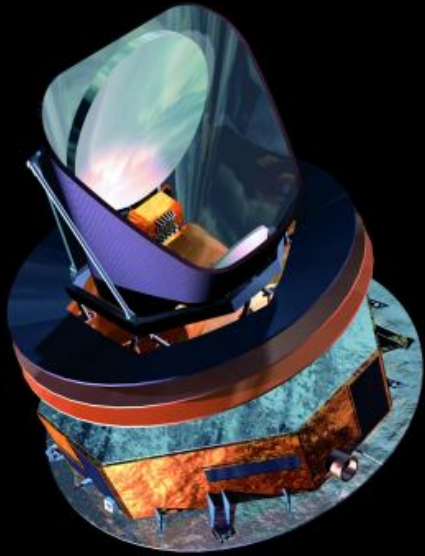
Frequencies: 30-1000 GHz

Square Kilometer Array (SKA)

Location: South-Africa or Australia

Start: 2015-2020

Frequencies: 0.1-10 GHz



 LOFAR

LOFAR

Location: Netherlands

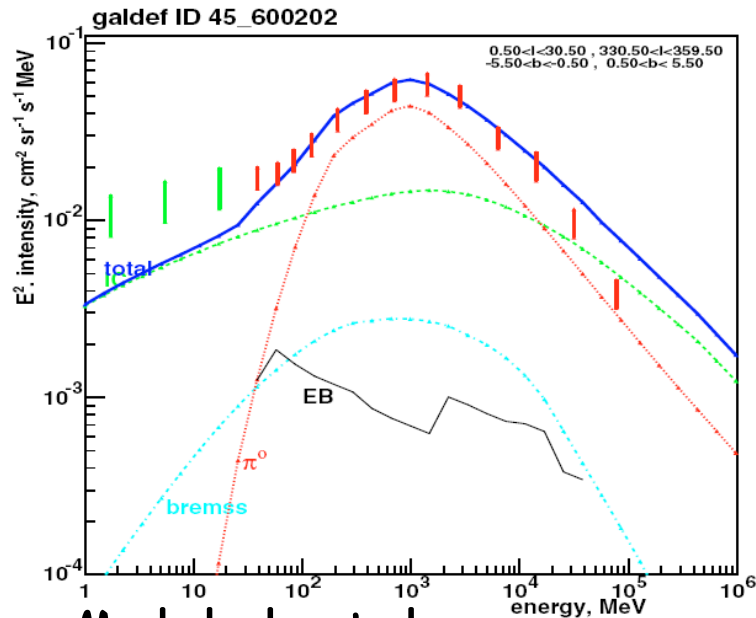
Completion: 2011

Frequencies: 40-200 MHz

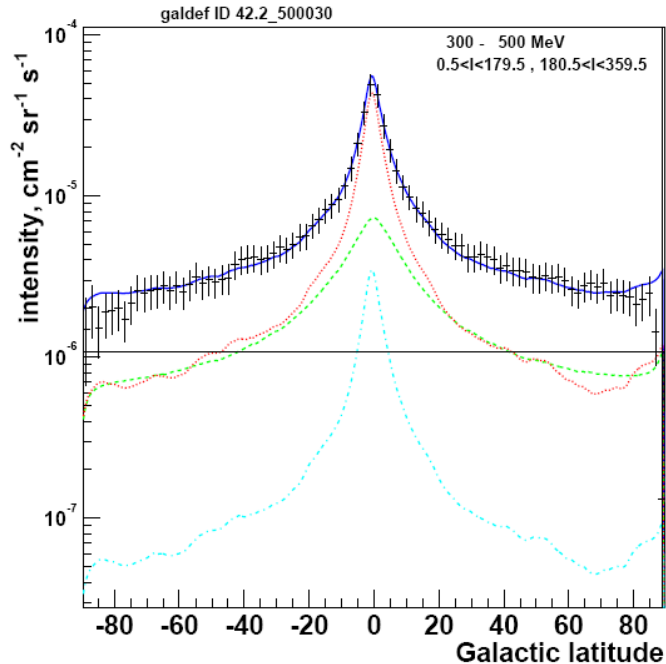


Milky Way Halo and Secondary Radiation: Inverse Compton

The Gamma Sky



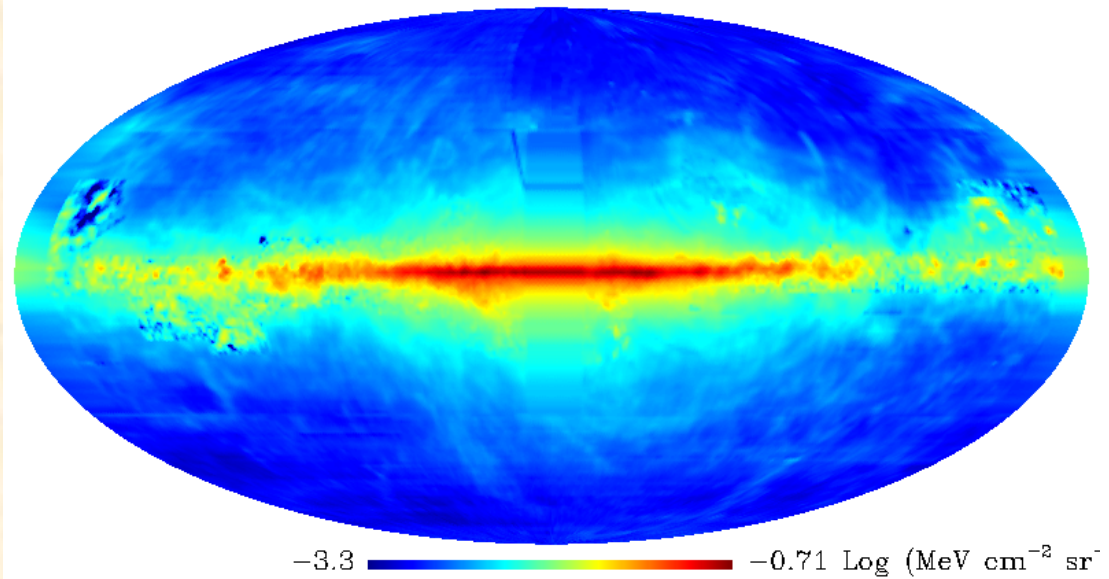
Moskalenko et al.



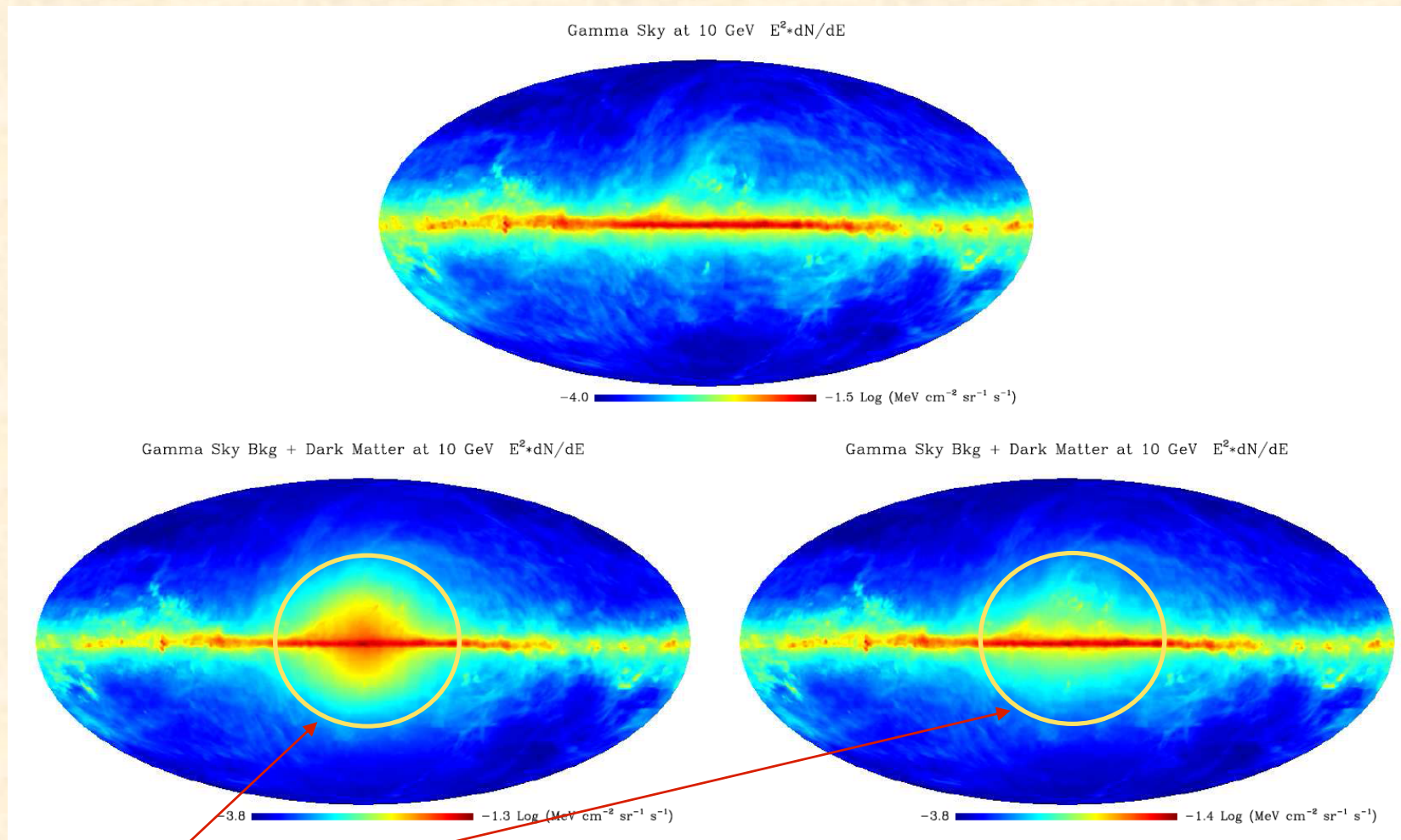
- Galactic Contribution from:
1. Pion Decay
 2. Inverse Compton
 3. Electron Bremsstrahlung

Galprop Foregrounds Model:

Gamma Sky at 1477.88 MeV $E^2 \cdot dN/dE$



The "ICS Haze"



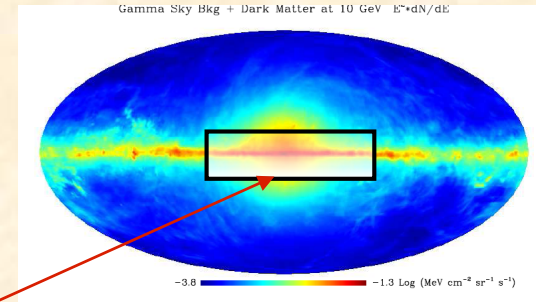
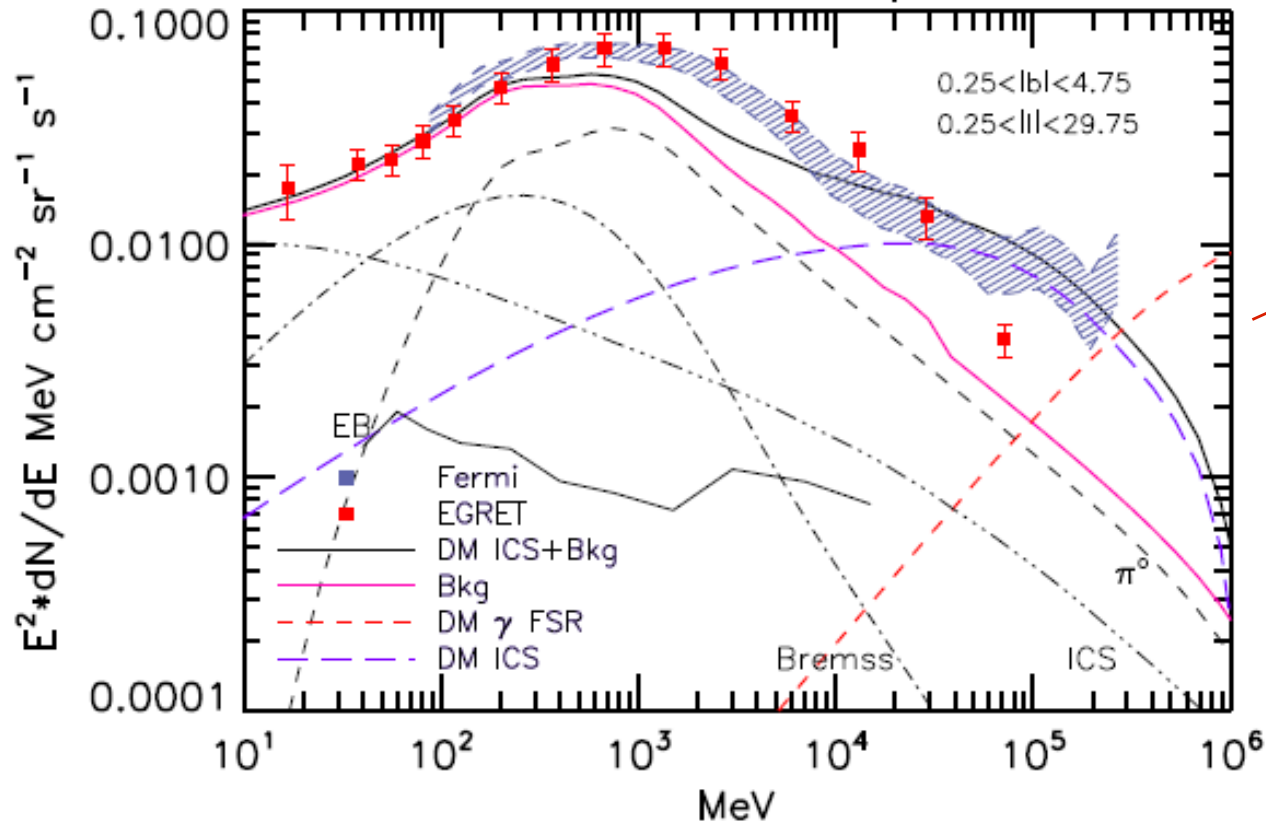
Similarly to the synchrotron case, IC signal produces an extremely peculiar "ICS Haze" peaking around 10-100 GeV which provides a further mean to discriminate the DM signal from the astrophysical backgrounds and/or to check for possible systematics.

ICS and background Spectra from Pamela/ATIC and forecast for Fermi



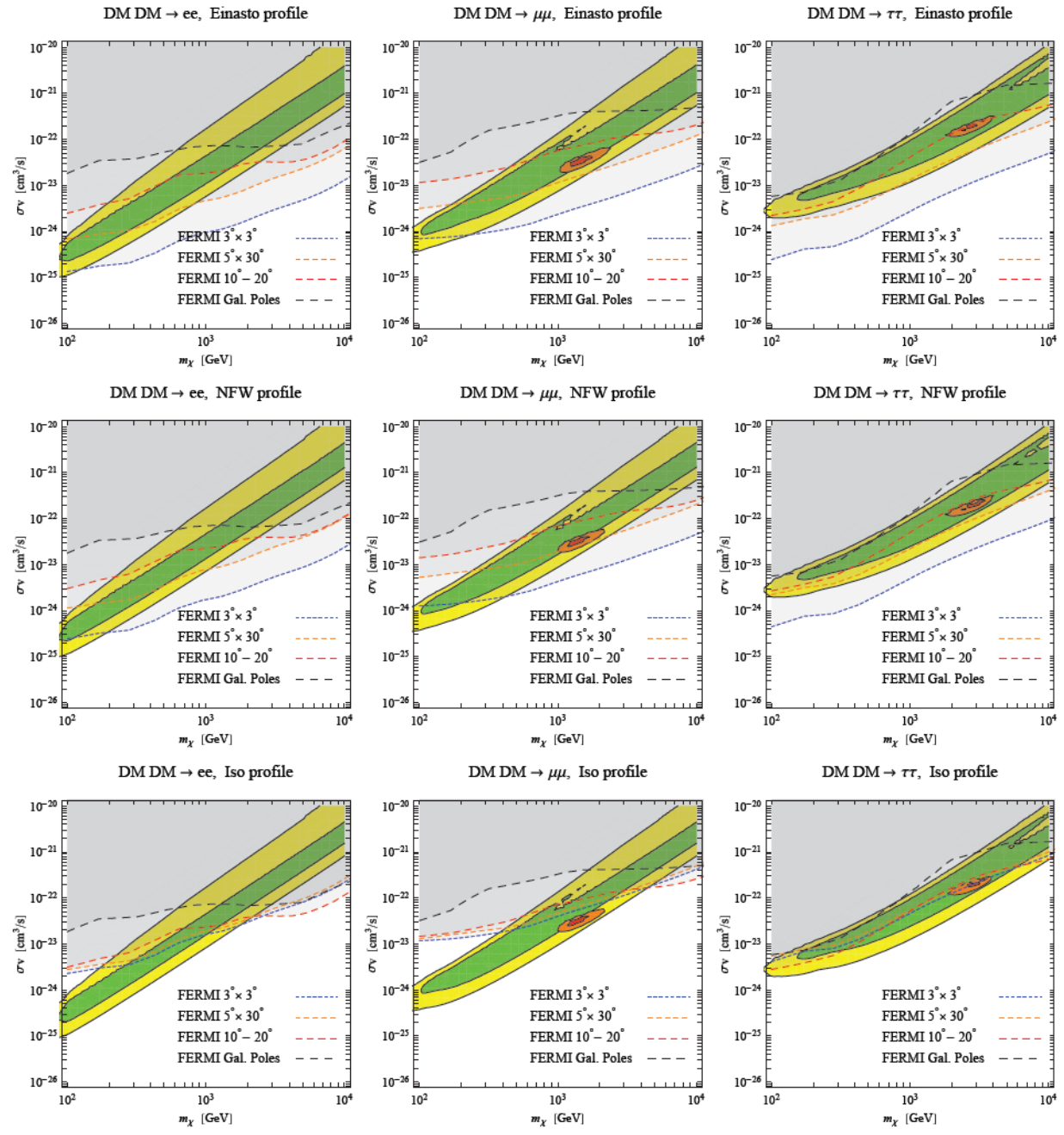
- The Pamela/ATIC electrons produce a large excess of Inverse Compton Radiation w.r.t to the galactic backgrounds
- EGRET somewhat disfavors the excess. Fermi can say more, but care is needed with the systematics

ICS and Gamma spectra



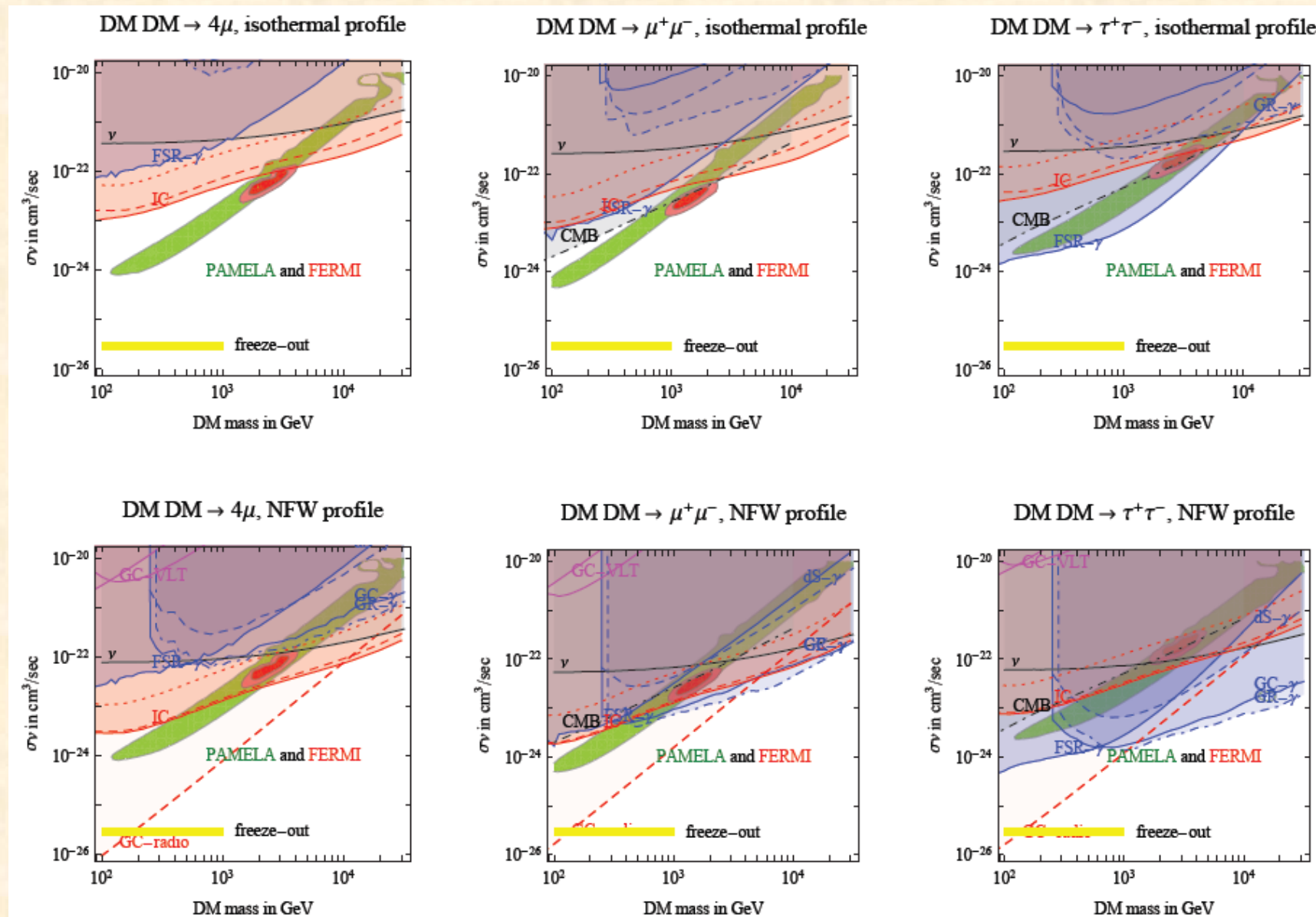
E. Borriello, A. Cuoco, G. Miele
Ap.J. 699: L59-L63, 2009

DM constraints from ICS and Fermi data

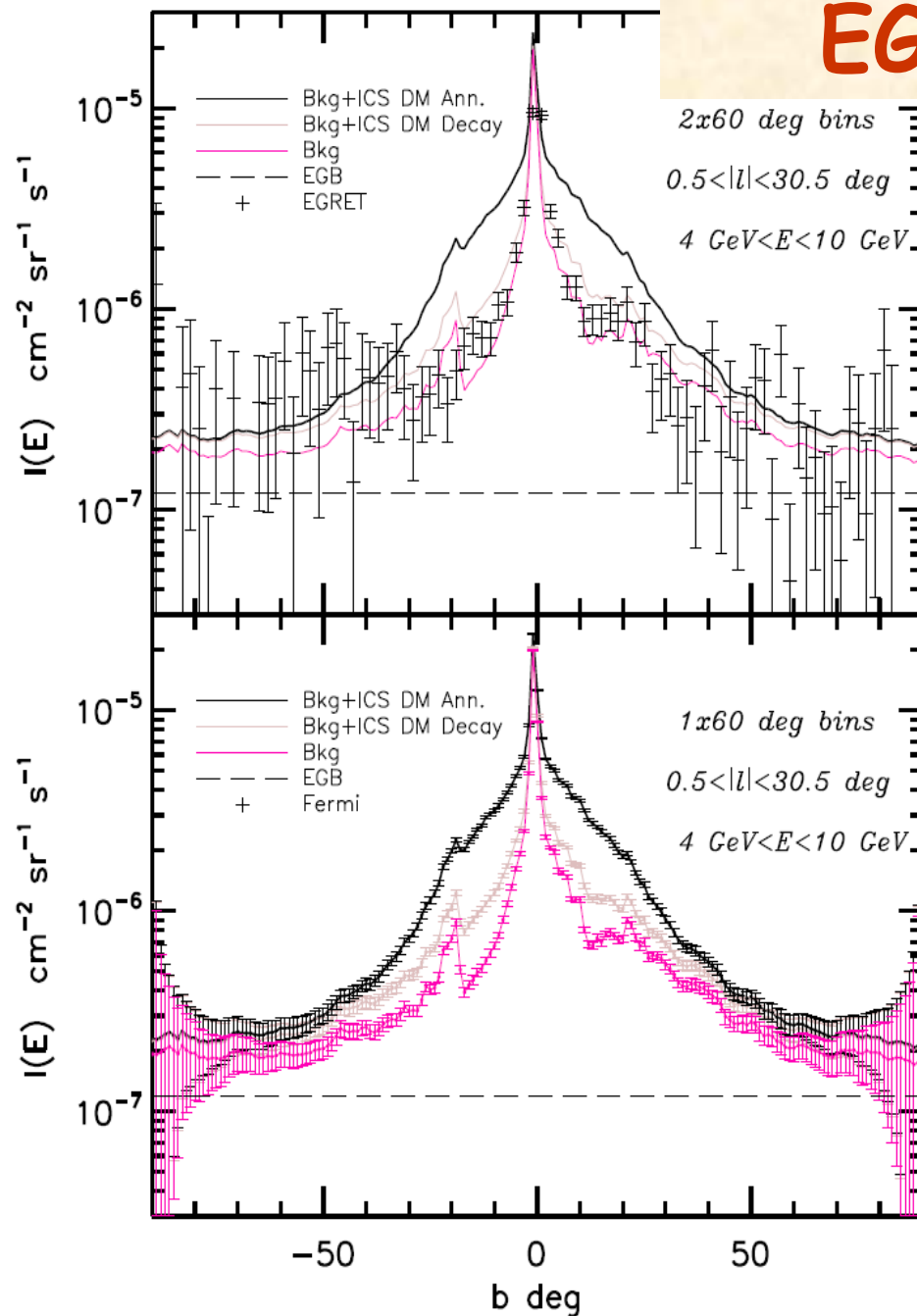


M. Cirelli, P. Panci, P. D. Serpico, arXiv:0912.0663

DM constraints from ICS and Fermi data



Profiles and Comparison of EGRET/Fermi Statistic



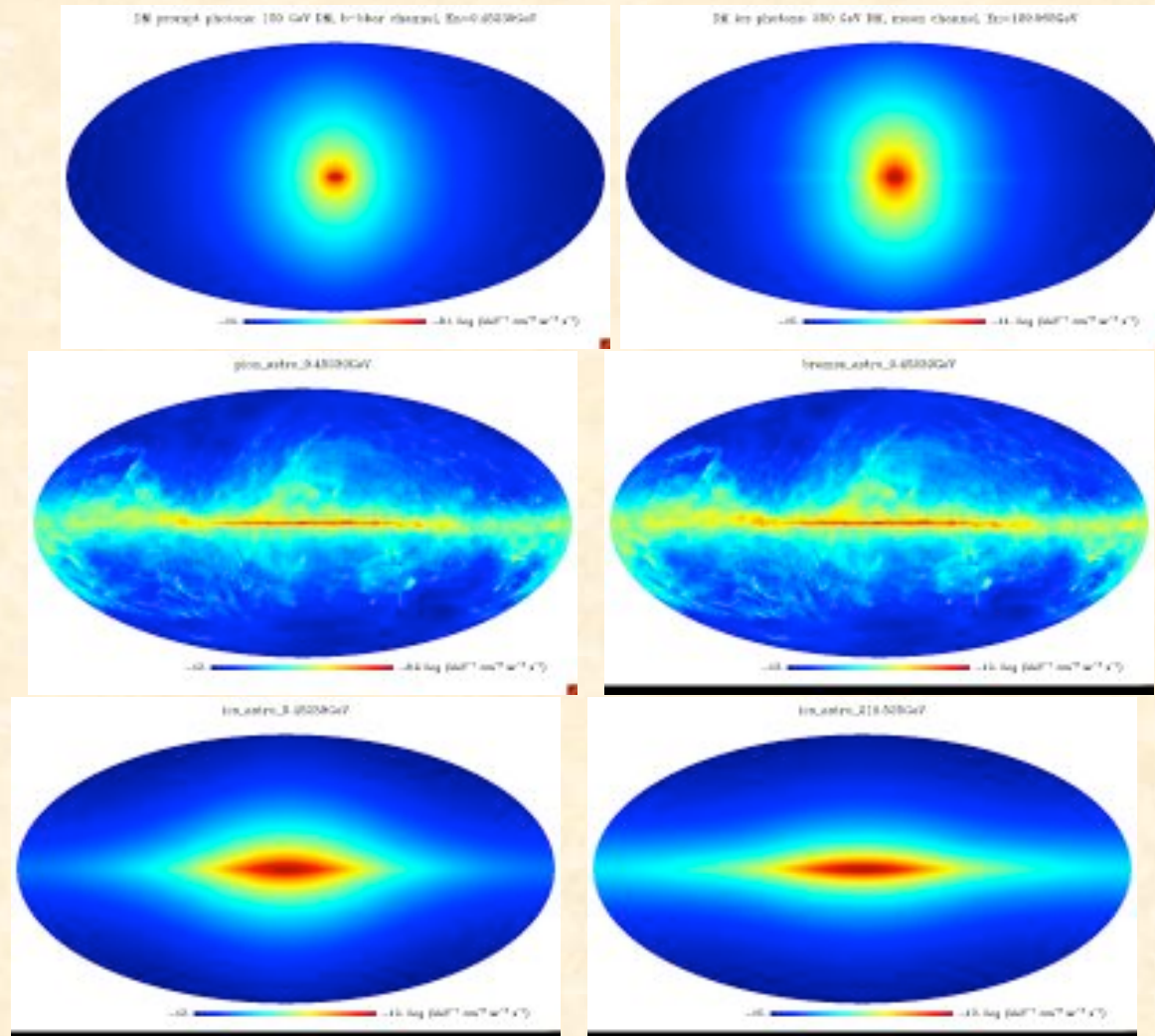
- Upper panel: EGRET data compared the annihilation model and the decaying model. Annihilating DM produces a too much broad peak to fit the data, beside producing an excessively high normalization.

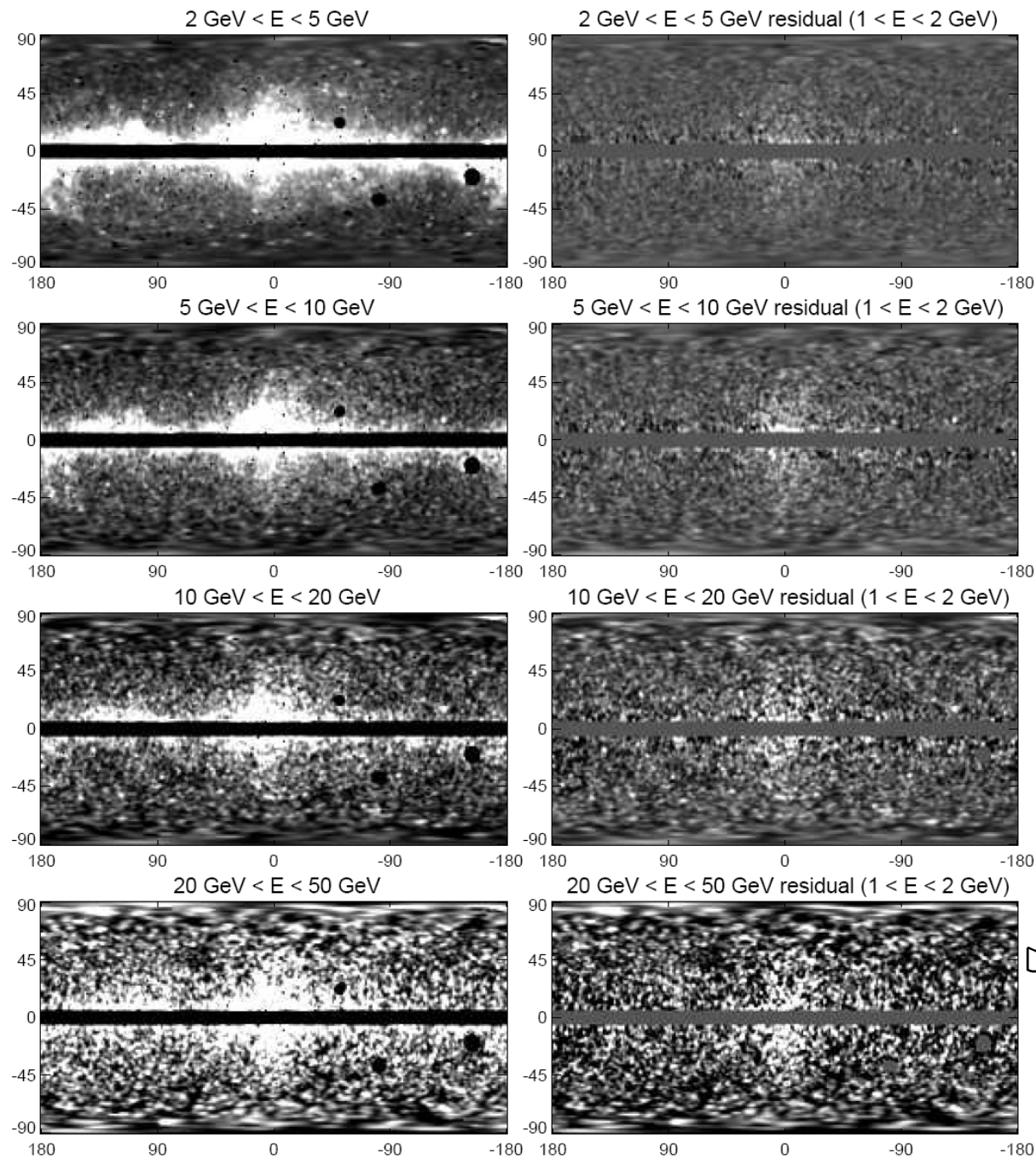
- Lower Panel: forecast of the Fermi ability to discriminate among the astrophysical and annihilating DM scenario. Also shown is the Decaying DM scenario.

Systematics:

- Uncertainties in the exposure
- Residual charged particle contamination.
- Foreground modeling

Morphology of the gamma-sky components





A Fermi Haze?

Dobler, Finkbeiner et al. 2009

FIG. 5.— The same as Figure 3 but using the *Fermi* 1-2 GeV map for cross-correlations instead. Unlike the SFD dust map which should trace π^0 emission only, the low energy *Fermi* map includes the soft ICS and bremsstrahlung associated with lower energy electrons. In fact comparing the residuals in this figure with those in Figure 3, it is clear that the disk component has been subtracted leaving only the ICS haze. Furthermore, the ICS haze is more prominent in the high energy maps indicating a harder spectrum than π^0 emission which is the dominant emission mechanism at ~ 1 GeV energies.

DM interpretation of the Fermi Haze

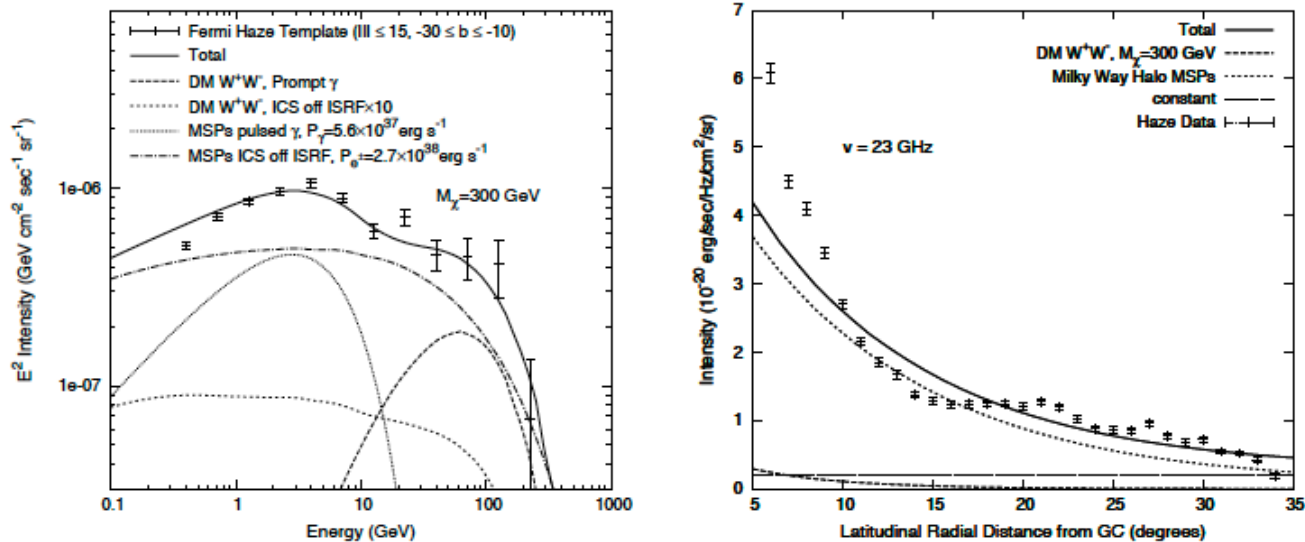


Fig. 1.— Left: contribution of pulsed γ -ray emission from MSPs, prompt γ -ray emission from annihilating DM, and ICS off MSP and DM electrons to the γ -rays haze spectrum. Right: corresponding contribution of the synchrotron radiation from the electrons to the microwave haze at 23 GHz. The parameters for the pulsed γ -ray emission are $n_\gamma = 1.3$, $E_{\text{cut},\gamma} = 4 \text{ GeV}$. The MSP e^+e^- injection spectrum parameters are $n_e = 1.3$, $E_{\text{cut},e} = 300 \text{ GeV}$. The dark matter has a mass $M_{\text{DM}} = 300 \text{ GeV}$ and annihilates into W^+W^- with $\langle\sigma v\rangle_0 = 3.0 \times 10^{-26} \text{ cm}^3\text{s}^{-1}$. The spacial distribution of MSPs and DM is discussed in the text. We use $R_c = 2 \text{ kpc}$ for the distribution of MSPs. The total power in pulsed γ -rays and in e^+e^- emission from MSPs is $W_\gamma = 5.6 \times 10^{37} \text{ erg/s}$ and $W_{e^\pm} = 2.7 \times 10^{38} \text{ erg/s}$ respectively. For a mean $\dot{E}_{\text{MSP}} \sim 2 \times 10^{34} \text{ erg/s}$ it corresponds to about 3×10^4 halo MSPs with average conversion efficiencies $\eta_\gamma \approx 0.1$ and $\eta_{e^\pm} \approx 0.5$.

Summary and Conclusions

- Secondary radiation provides a complementary mean to test/find possible DM signatures.
- Secondary Radiation and Final State Radiation in particular provides a fairly model independent test of the origin of the PAMELA/ATIC/FERMI electrons.
- Fermi data provide already interesting constraints on DM . More statistics and a study of the foregrounds can further pin down the limits.